Thrust-Reverser Investigation by Large-Scale 3D PIV

Hysa, I.; Tuinstra, Marthijn; Lammers, K; Scarano, F.; Sciacchitano, A.; Gebbink, Roy; Harrison, C

DOI
10.2514/6.2022-1945

Publication date
2022

Document Version
Final published version

Published in
AIAA SCITECH 2022 Forum

AIAA SciTech Forum
January 3-7, 2022, San Diego, CA & Virtual
AIAA SCITECH 2022 Forum

10.2514/6.2022-1945

Thrust-Reverser Investigation by Large-Scale 3D PIV

Hysa, Ilda[1]; Tuinstra, Marthijn[2]; Lammers, Karel[3]
Netherlands Aerospace Center NLR, Marknesse, 8316 PR, the Netherlands

Scarano, Fulvio[4]; Sciacchitano, Andrea[5]
Delft University of Technology, Delft, 2629 HS, the Netherlands

Gebbink, Roy[6]
German-Dutch Wind Tunnels DNW, Marknesse, 8316 PR, the Netherlands

Harrison, Charles[7]
Gulfstream Aerospace Corporation, Savannah, GA, 31408 USA

Volumetric PIV measurements are performed to study the flow development around a 1:12 scale model of a thrust reverser in a low-speed wind tunnel. The thrust-reverser operates in a freestream flow of 3-5 m/s and with a jet to freestream velocity ratio V_{jet}/V_{inf} ranging from 1.5 to 6. Making use of sub-millimeter helium-filled soap bubbles, large-scale PIV measurements are performed that encompass a 3D domain of approximately 0.4 m^3. The flow exiting the thrust-reverser features two inclined jets that interact with the wind tunnel free stream, the nacelle, fuselage and ultimately the tunnel walls. Such interactions result in highly three-dimensional patterns and jets large scale fluctuations. The jet reversal characteristics with varying freestream velocity and nozzle pressure ratio are characterized quantitatively. The work demonstrates the feasibility of quantitative inspection of the flow behavior in a three dimensional domain for industrial applications.

I. Nomenclature

PIV	=	particle image velocimetry
HFSB	=	helium-filled soap bubbles
NLR	=	Netherlands Aerospace Center
AWT	=	Aero-acoustic Wind Tunnel
TR	=	thrust reverser

[1] PhD candidate, Aerospace Engineering TU Delft/ Vertical Flight and Aeroacoustics department NLR, e-mail : ilda.hysa@nlr.nl
[2] Scientist Principal, Vertical Flight and Aeroacoustics Department
[3] R&D Engineer, Vertical Flight and Acoustics Department
[4] Professor, Aerodynamics Department
[5] Assistant Professor, Aerodynamics Department
[6] Projects Manager, Projects Department
[7] Technical Specialist, Flight Dynamics

NPR = nozzle pressure ratio
STB = Shake-the-Box

II. Introduction

Aircraft engine thrust can be redirected by thrust reverser (TR) devices to modify the direction of the propulsive force and to rapidly decrease the aircraft speed at landing, after touchdown. The flow resulting from angling the thrust vector loses the quasi-axial symmetry, to become highly three-dimensional, in turn involving large separated regions and unsteady behavior. During aircraft operations, the behavior of TRs can be critical not only to ensure sufficient air-breaking [2], but also to avoid unwanted exhaust re-ingestion [3] or potential interference with control surfaces at the wing or tail segments [1]. Therefore, the full characterization of these complex mechanisms is necessary in order to make accurate predictions leading to design optimizations of TRs. The aerodynamic design verification of such systems relies upon a combination of wind tunnel measurements and numerical simulations.

Bryanston-Cross and Sale [4] characterize the flow leaving the thrust reverser kicker plate by means of planar PIV measurements. Exception made for this study, most reported works that deal with thrust-reversers in wind tunnels make use of more traditional methods, namely force balance [2][3],surface pressure measurements [3][5] or qualitative smoke or stream visualization [1].

An important phenomenon in thrust reverser studies is the unwanted plume re-ingestion, whereby, the engine exhaust flow recirculates upstream and is captured again at the inlet. This negatively affects the engine lifetime and performance. A way to check for re-ingestion involves measuring the temperature in the engine inlet, based on the assumption that the exhaust air flow that is reversed is hotter than the free stream [3]. Flow visualization techniques provide immediate and intuitive approach to this problem, and have been employed to study some details of the flow field topology. Van Hengst [1] made use of surface tufts to detect separation lines on the nacelle. Additionally the reversed jet plume was visualized by vaporizing liquid nitrogen, as well as by steam injection [1]. Amin and Richards [5] also conducted visualization experiments in a water tunnel, injecting colored dye into the reverser jet as a visualization technique, and comparing it to mist visualizations in the wind tunnel. The aforementioned visualization methods were effective to deliver a qualitative insight into the overall flow behavior and topology, however the detailed analysis of specific planes of interest is hindered by the fact that only the plume surface is visible. Moreover, comparison among experiments or with data obtained from numerical simulations is hampered by the qualitative nature of the observation.

Over the past decade particle image velocimetry (PIV) has matured from its developmental stage to a reliable whole field measurement technique, which makes it a powerful tool in industrial aerodynamic research. Despite its advancements, the application of PIV in aeronautics poses a number of technical challenges: the region of interest often exceeds the size of the available observation areas (due to limitations in illumination and camera resolution); restricted access around complex objects often requires multiple rearrangements of the illumination and imaging systems; the above poses significant time constraints in the setup of the PIV system, conflicting with the high operational costs of large wind tunnels.

The challenge of large measurement domains has been addressed by the introduction of neutrally buoyant tracers of sub-millimeter diameter: helium-filled soap bubbles (HFSB). Techniques to produce a large amount of HFSB and distribute them in the wind tunnel stream have been refined in recent years [6]. The control of HFSB properties at generation and their aerodynamic fidelity in wind tunnels is documented in the works of Faleiros et al. [7] and Gibeau and Ghaemi [8]. Using HFSB, Faleiros et al [9] successfully conducted stereoscopic PIV measurements in the wake of a tilt-rotor aircraft at the Large Low-speed Facility (LLF) of the German-Dutch Wind tunnels (DNW) encompassing a field of view (FoV) of 1.1 x 1.1 m^2. Employing a specially designed rake of 9 m^2 area, this experiment indicates the upper practical limit to date for tracers concentration that can be achieved in an industrial environment by this technique. Industrial testing demands for increases in information density in order to increase the data productivity of wind tunnel experiments. This can be achieved by turning from planar to 3D (volumetric) measurements, which also offer the opportunity to extend the amount of information that can be extracted from the dataset, most notably pressure (pressure from PIV, [10]).

A volumetric PIV method that addresses the challenge of optical access and time constraints in the setup of the PIV system is robotic volumetric velocimetry, introduced by Jux et al. [11], based on the concept of coaxial volumetric velocimetry (CVV) [12]. This approach was recently used by Sciacchitano et al. [13] to perform quantitative flow measurements around a turboprop aircraft at the Low-Speed Tunnel (LST) of DNW, where a measurement volume of 0.15 m^3 was covered. Albeit its potential as a volumetric measurement technique, the aerodynamic intrusiveness of

the robot arm in the flow needs to be evaluated case by case. Furthermore, the limited tomographic aperture of the CVV system, yields velocity vector measurements with disparity in the uncertainty along the different components.

Instead large-scale, full-field tomographic particle tracking velocimetry (PTV) experiments offer the potential to accurately yield the instantaneous 3D velocity field. Experiments conducted by Vidales et al. [14] in the LST, DNW have made use of this technique, employing HFSB as flow tracers and four high speed cameras for the imaging. A measurement domain of approx. 0.2 m^3 was surveyed in the study of the flow on the landing deck of a simplified frigate shape model.

In the present work 3D PIV measurements are performed in the Aero-acoustic Wind Tunnel of the Netherlands Aerospace Center (AWT, NLR) around a thrust reverser system. The 3D PIV technique is used in order to cope with the complex three-dimensional topology of the flow when the thrust reverser is operated. The current work aims at combining the whole field character of flow visualization experiments, with the quantitative nature of PIV. The large-scale PIV technique is therefore deployed and demonstrated in this complex flow and within the time constraints dictated by the industrial environment.

III. Experimental apparatus and measurement conditions

A. Wind tunnel and TR model

Experiments are performed in the aero-acoustic wind tunnel at the National aerospace laboratories (NLR-AWT). The facility features a 0.95 x 0.95 m^2 closed test section of 1.9 m length, with plexiglass walls for extended optical access. The wind tunnel is operated in the speed range 3-5 m/s. The thrust reverser is of the blown nacelle type, the model is a G500, implemented on the Gulfstream G500 aircraft designed and manufactured by Gulfstream Aerospace. The model is on a 1:12 scale, with nacelle full length of 52 cm, maximum diameter of 15 cm and with a fixed TR door angle configuration. It is installed at 20 cm from the wall and 56 cm from the floor. Fig.1 shows the model mounted in the wind tunnel, along with the coordinate system used for the image analysis. Table 1 summarizes the dimensions of the TR model length l_{TR}; the fuselage-like body to which the TR was attached l_{fb}; the angle the upper thrust reverser door makes with the horizontal θ_1; the angle the lower TR door makes with the horizontal θ_2; and the dimensions of the measurement volume in the x, y and z directions: l_x, l_y, and l_z respectively.

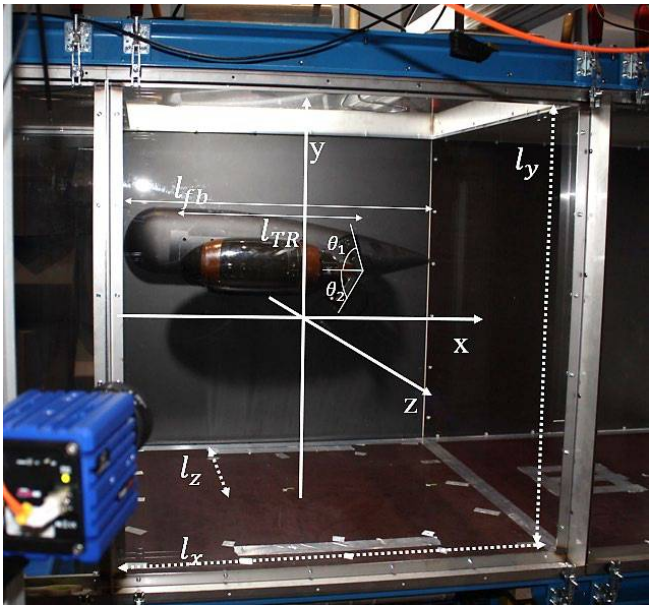

Fig.1 TR model in the test section of the AWT, with indication of relevant geometrical parameters

TR model dimensions	
l_{TR} [mm]	520
l_{fb} [mm]	930
θ_1 [deg]	71
θ_2 [deg]	74
Measurement volume dimensions	
l_x [mm]	950
l_y [mm]	950
l_z [mm]	450

Table 1 Dimensions of the TR model and measurement volume

Fig.2 shows a photograph of the experimental setup, illustrating the positions of the laser and cameras with respect to the measurement volume around the TR model.

Pressurized air is used to simulate the thrust reverser jet. The compressed air supplied to the TR is not heated and the buoyancy effects are negligible. The flow in the test section throughout the experiment is approximately isothermal. The nozzle pressure ratio i.e. the ratio between the total pressure at the nozzle inlet to the static pressure of the free stream (NPR) was measured real-time and the input voltage to the pressure regulator was set to achieve the desired NPRs. The maximum achievable NPR was 1.0127. The engine suction was not simulated in this experiment.

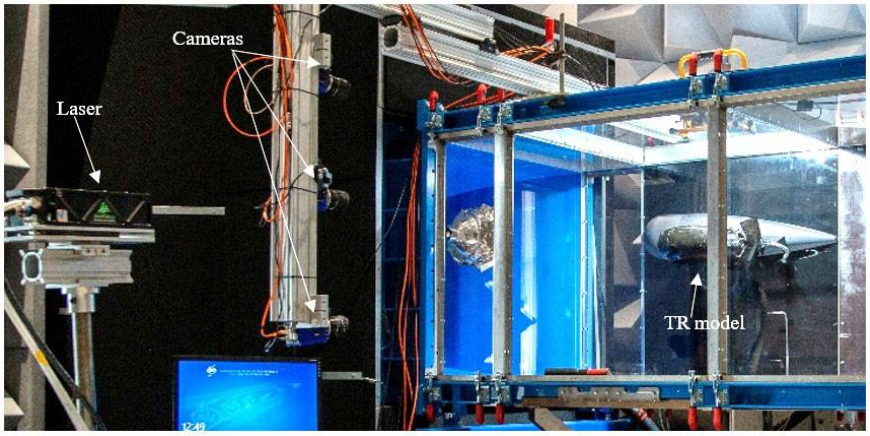

Fig.2 Photograph of the test setup

B. PIV apparatus and procedures

B.1. Seeding system

The flow is seeded with neutrally buoyant HFSB of median diameter of 0.45 mm. The tailor-made seeding rake is shown in Fig. 3. As the rake is placed inside the nacelle measurements were made to quantify the rake's aerodynamic interference on the internal nacelle flow. Test points with and without the HFSB rake were performed to investigate the effect on the total pressure distribution within the nacelle. It was found that the presence of the rake results in approx. 5% total pressure drop, which translates into a 5% lower NPR from the intended value. Accordingly, the set NPR was adjusted for this loss.

The rake comprises 8 generators that can deliver tracers at a total rate of 300×10^3 bubbles/s. The fluid supply unit is operated such that the flow rates for each generator are: air – 100l/h, He – 9l/h, soap – 10 ml/h, a condition expected to deliver monodisperse neutrally buoyant tracers [7]. Only the exhaust flow is seeded, resulting in inhomogeneous seeding conditions across the measurement domain. Fig. 4 illustrates the seeded region of the measurement domain.

Fig. 3 HFSB rake with the 8 generators. The transparent capillaries carrying helium, soap and air can be seen in the back

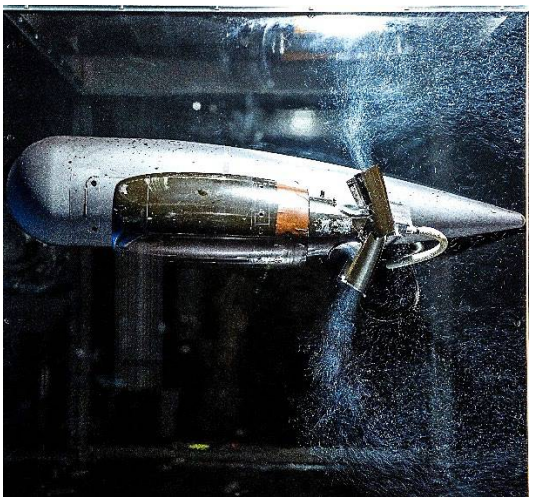

Fig. 4 Photograph of the TR model in the test section. The HFSB particle streaks are visible within the seeded jets.

B.2. Illumination

A Quantel Evergreen 200 Nd:YAG laser (2 x 200 mJ/pulse at 15 Hz) is used as a source for the particles illumination. The expansion of the laser beam by a spherical lens was found to create a speckle pattern. This phenomenon is mentioned by Raffel et al. [15], and it is produced by the interference of coherent wavefronts. As this pattern results in a non-homogeneously lit background, it is best avoided. The problem resides in the coherence of the beam, so the solution is to diffuse the light such that it becomes incoherent. This was achieved by shooting the beam into a piece of foam material, and then directing it to the measurement volume by use of a spherical mirror. The laser illumination direction is from the same side as the cameras viewing, resulting in the particles being illuminated at an angle of 20 degrees relative to the imaging direction.

B.3. Imaging and recording

The measurement system comprises three sCMOS cameras (pco.edge 5.5, 2560 x 2160 pixels, 16 bits). The cameras are equipped with f=35 mm objectives, set at an aperture f# = 8, yielding sufficient depth of field to image the volume with 45 cm depth. The cameras are arranged in a line configuration subtending a total angle of 25 degrees. The cameras are placed at 2.2 m distance from the TR model, with a magnification M = 0.0175 (0.37 mm/pixel), capturing a field of view of 0.95 x 0.95 m. The observed maximum velocities of up to 20m/s correspond to a particle shift that amounts to 0.4 mm (approx. 10 pixels). The measurements sequences of 1000 recordings are acquired at a rate of 15 Hz and with time separation Δt = 200 μs (spanning a duration of approx. 67 seconds of measurement per data point). Image acquisition, synchronization of cameras and the light source were achieved with a programmable timing unit (PTU X) and controlled by a PC with *DaVis* 10.1.2 software (LaVision). Table 2 summarizes the measurement parameters.

Parameter	Value
Laser pulse separation [μs]	200
Recording frequency [Hz]	15
Active sensor size [pixels]	2560 x 2160
Image sensor pixel pitch [μm]	5.6 x 5.6
Magnification	0.0175
Object focal length [mm] and aperture f#	35, 8
Measurement domain [m^3]	0.95 x 0.95 x 0.45

Table 2 Volumetric measurement conditions

The imaging of HFSB by the two glare points is discussed by Caridi [25], and the merging of glare points for large scale PIV (small M) by Faleiros [9]. In the current measurement configuration (Fig.2) with an angle between the illumination and imaging directions of approximately 20 deg, the tracers of 0.45 mm diameter will form glare points viewed with approximately 80 μm separation according to Faleiros [9]. In the present imaging conditions (f# = 8), the glare points merge within the diffraction disc of the imaging system.

The image-to-object space mapping function is obtained performing a 3D calibration procedure shifting a planar calibration target across three positions separated along the plane-normal direction by 130 mm. The final accuracy of the calibration was enhanced using Volume-Self Calibration [16] reducing residual disparity below 0.1 pixels. The latter was obtained with the same software as the geometric calibration.

B.4. Image pre-processing

Efficient detection and tracking of individual particle tracers requires minimal background light intensity. This is achieved by image pre-processing. Background intensity is reduced by applying a minimum subtraction filter applied over time, subtracting a constant value of 50 counts from each pixel, and then subsequently multiplying each pixel by a factor of 10. This was followed by applying a Butterworth high pass filter [18], which attenuates the undesired laser light reflections from solid objects. Fig.5 shows the raw and pre-processed images side by side, with significant attenuation of background illumination.

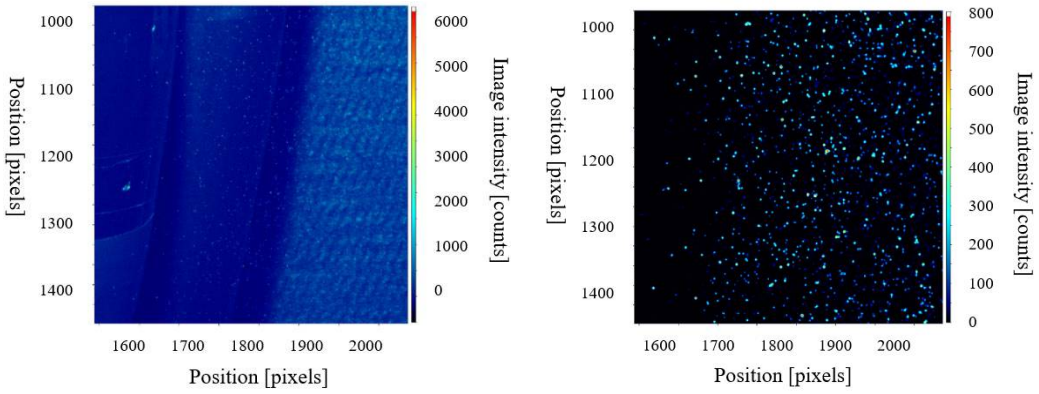

Fig. 5 Samples of raw image (left) and pre-processed image (right)

B.5. Data processing

The motion of the particles is evaluated using the Shake-the-Box algorithm tailored to two-pulse recordings, implemented in LaVision *DaVis 10.1.2* software. [19]. The instantaneous velocity is sampled at sparse locations and is converted to a Cartesian grid by locally averaging the velocity vector over cubic bins [20]. The number of samples contained in each cell depends upon the size and the local value of the tracers concentration. The chosen bin size is 26 mm and an overlap of 50% yields a vector pitch of 13 mm. The measurement spatial dynamic range (DSR) is estimated as the ratio between the domain larger size and the bin size, and it equals approx. 40. The dynamic velocity range is estimated as the ratio between maximum and minimum measured tracers velocity and is equal to approx. 35. Table 3 summarizes the data processing parameters.

Parameter	Value
Spatial resolution [mm]	26
Vector pitch [mm]	13
DSR	40
DVR	35

Table 3 Data processing parameters

Considering the root-mean-square of the velocity standard deviation in a bin, the standard uncertainty of the mean is given by [20] :

$$\overline{\sigma_u} = \frac{\sqrt{\sigma_u{}^2}}{\sqrt{N_p}} \qquad (1)$$

Further post-processing of the time-averaged binned velocity vector fields is performed in *Tecplot* 360 EX R2. The volumetric vector fields are overlaid onto a CAD of the TR model, where desired aspects of the flow are highlighted accordingly.

IV. Data reduction

A. Global flow topology

The results indicate that the flow through the reverser is of highly three-dimensional nature. The time-averaged velocity field of the flow around the nacelle is illustrated in Fig. 6. The streamlines, color-coded by the streamwise velocity component reveal a multitude of large-scale structures. The reversed jet from the thrust reverser consists of two main jet plumes. The forward penetration of these plumes and their interaction with the tunnel walls gives rise to two large regions of flow recirculation. As the nacelle is not mounted symmetrically but is closer to the upper wall the recirculation in that region is stronger and representative of the ground effect (note that the TR is mounted upside down) [5]. The other jet plume, namely the lower plume as shown in Fig.6 would ideally be representative of the jet expanding into free air, however a recirculation region is noted on this side as well, a byproduct of the presence of the tunnel wall due to the closed test section. At the shown condition of free-stream velocity of 5 m/s and NPR of 1.012, there is evidence of beginning of re-ingestion due to the ground effect recirculation, although it has to be noted that the detailed study of re-ingestion characteristics requires a realistically simulated engine. Evidence of flow leakage, i.e. the flow escaping from the gap existing behind the deployed TR doors [3], is also detected.

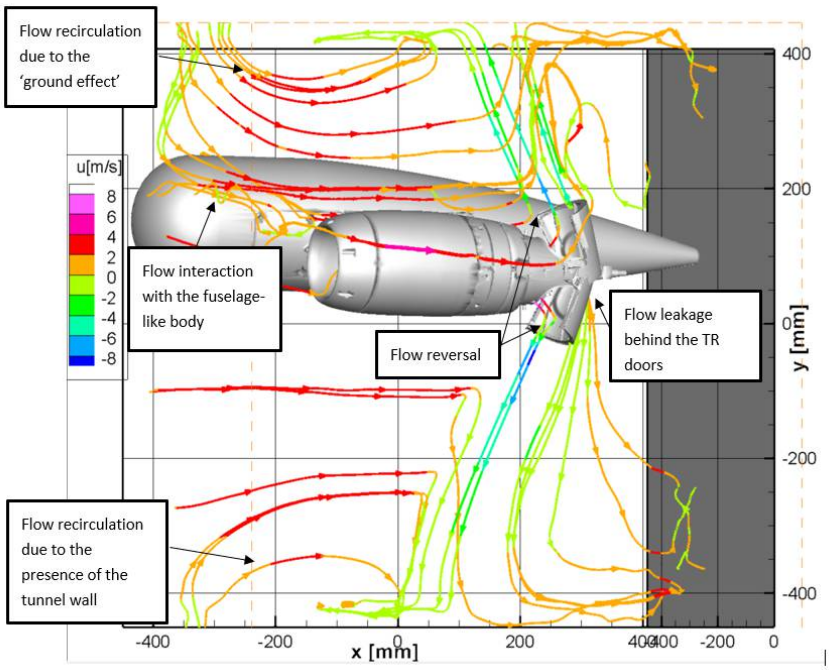

Fig. 6 Global features of the velocity distribution around the TR model, V_{inf} = 5 m/s, NPR = 1.012

B. NPR effect on the jet velocity distribution

A comparison between the different data points with different freestream velocity and NPR gives an impression of the jet properties variation. For the current configuration of fixed TR door angles, the upstream penetration of the reverser plume depends on the ratio of the jet momentum to freestream momentum [5], and considering the low speeds at which the experiment was conducted, the flow can be assumed to be incompressible.

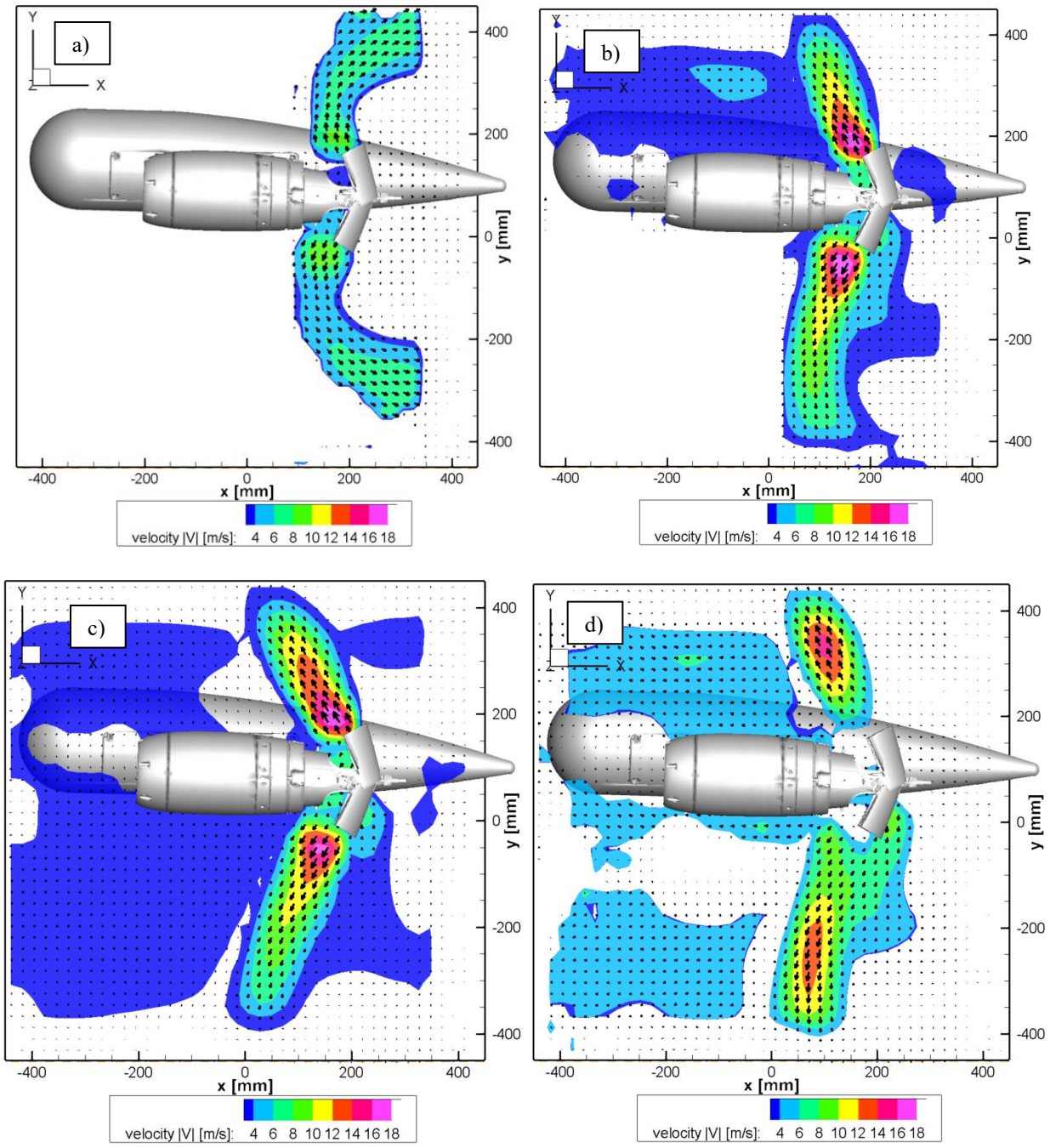

Fig. 7 Velocity contours and streamwise velocity vectors plots at the mid-plane through the TR

a): V_{inf} = 5 m/s, NPR = 1.0015; b): V_{inf} = 5 m/s, NPR = 1.0055;

c): V_{inf} = 3 m/s, NPR = 1.0055; d): V_{inf} = 5 m/s, NPR = 1.012

Comparing the results from the conditions presented in Fig.7 in cases a), b), and d) with same freestream velocity but different NPR, it is clear that the NPR increase results in jet momentum increase. The shift follows from a condition of no flow reversal as in a), to a transition phase in case b) where the upper plume reverses and moves further upstream, while the lower plume is not fully reversed, to full reversal in case d). Note that, since the exterior flow was not seeded, the presence of tracer particles outside of the jet, i.e. ahead in the region adjacent to the nacelle and tunnel walls as can be clearly observed in cases c) and d), and only for the upper half in case b), is due to the interaction of the jet with the freestream.

Similarly comparing cases b) and c), for the same NPR and similar values of jet momentum, the decrease in freestream momentum from b) to c) gives rise to stronger reversal.

Although the effect of the modification of the flow field due to inlet suction is not captured in this study, it can be noticed that in conditions c) and d), the reversed plume penetrates upstream further than the engine inlet station, which seems to signify onset of re-ingestion. A summary of forward jet penetration for five data points with different conditions is presented in Table 4. The data points that reach the engine inlet can be considered as a preliminary warning for the onset of re-ingestion, however as stressed earlier further study is required to conclude on this point.

Measurement Condition	**Jet upstream penetration**
V_{inf} [m/s], NPR	x/x_{inlet}
5, 1.0015	0.2
5, 1.0055	~1 *
4, 1.0055	1
3, 1.0055	1.2
5, 1.012	1.2

* the jet plume interacting with the ground only

Table 4 The forward penetration of the reversed jet with different measurement conditions ($x/x_{inlet} = 0$ corresponds to the TR doors location, $x/x_{inlet} = 1$ to the engine inlet)

C. Jet plumes symmetry

It is important to keep in mind that the lower plume corresponds to the jet expanding into free air, and the upper plume to the one interacting with the ground. As far as jet axial symmetry is concerned it seems difficult to generalize. For the cases a) and c) presented in Fig.7, the jet seems to retain a fair degree of axial symmetry, but this does not hold for the other conditions. In all cases b), c) and d) the lower jet plume extends further in the y-direction, consistent with the lack of hindrance from the tunnel wall that is further away in that direction. Consequently the lower plume appears to be thinner and slightly slower at the centre.

From Fig.9 it can be noted that the jet cross section is closer to being symmetric in the proximity of the doors, and becomes increasingly asymmetric as it progresses upstream. This observation is attributed to the slight geometric differences between the two different doors, in combination with the different distance to the tunnel walls. It can be observed in Fig.9 in both cases e) and f) that the upper plume, i.e. the plume closer to the wall simulating the ground effect is faster at the center, and the lower plume expanding into a larger open region is more diffused and slower at the center.

D. Measurement uncertainty estimation

The turbulence levels of the wind tunnel test section are $T_{ux} = 0.03$ %, $T_{uy} = 0.02$%, and $T_{uz} = 0.013$%. As discussed earlier, the seeding is non-homogenous, so after the image processing the density of the tracks identified is also a function of the spatial position. Fig.10 shows the number of tracks per cm^3 plotted in the x-y midplane through the thrust reverser for a datapoint with $V_{inf} = 3$m/s and NPR = 1.0055 (the condition depicted in Fig.7c)). Note that as this is a double-frame measurement the tracks are equivalent to the velocity vector samples.

The time-averaged concentration of tracks is highest close to the TR doors as expected, decreasing further upstream. It can be observed that the region between the nacelle and the upper tunnel wall is more densely seeded as compared to the region bounded by the lower wall.

It is discussed by Caridi et. al [24] that the seeding concentration in large-scale PIV is inversely proportional to the flow velocity at the location where the tracers are released, which in this case corresponds to the velocity at the

nozzle inlet, and is therefore a function of the NPR. A study of the differences in tracers concentration between the different conditions revealed that the tracers concentration in the jet region exceeds $2x10^4$ particles per bin even in the case of the highest freestream speed and NPR tested (V_{inf} = 5 m/s, NPR = 1.012), and exceeds 1000 particles per bin in the regions surrounding the jet.

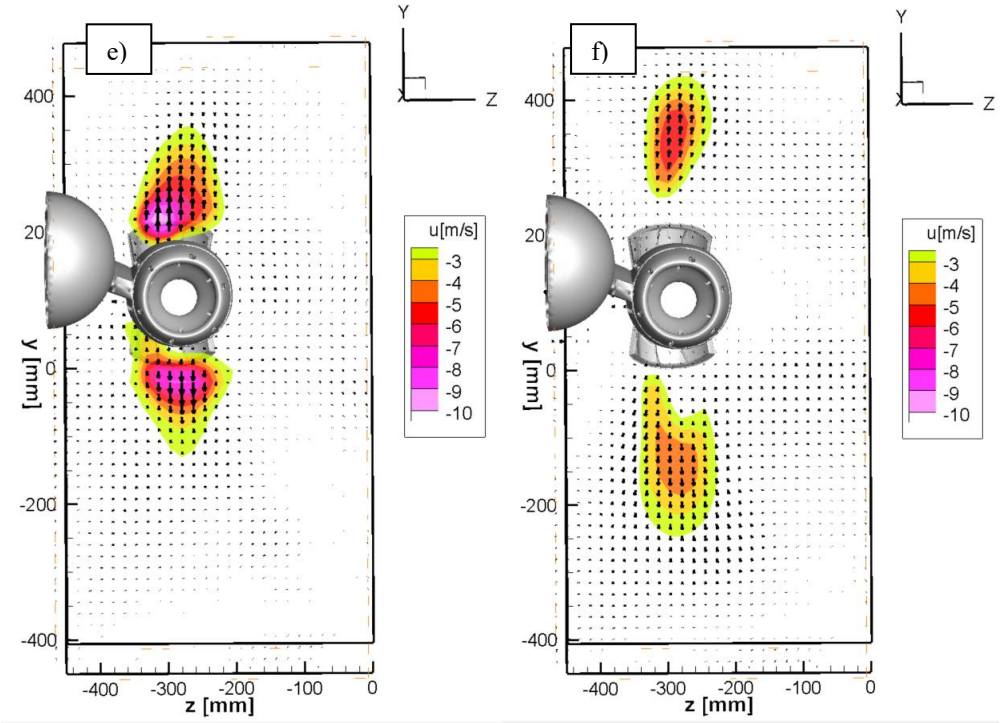

Fig. 9 e): Streamwise velocity contour on a yz plane 30 mm upstream of the TR doors; f): Same plot 100 mm upstream of the TR doors ; V_{inf} = 3 m/s, NPR = 1.0055

Measurement uncertainty as defined by Eqn.1 inside the jet plume – in the point denoted by a cross in Fig.10 - is found to be less than 0.1% of the peak absolute velocity measurement. This is because the relatively large amount of tracers in the jet region decreases the uncertainty of the measurement in the jet center.

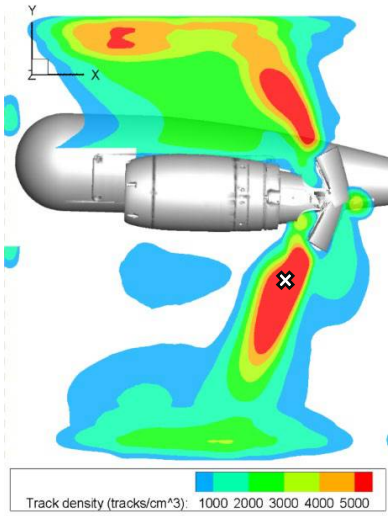

Fig. 10 Track density in the x-y midplane through the thrust reverser (V_{inf} = 3m/s, NPR = 1.0055).

As can be observed from Fig. 10, the number of samples in the midplane through the nacelle is a function of the distance from the jet center. The same holds for the depth dimension (the out of plane coordinate in Fig.10), such that the further one moves from the TR doors in the z direction, the smaller the particle concentration, decreasing to a minimum in the edges of the jet. It was found that the measurement uncertainty in the extremities of the plume along the z- direction increased to around 1% of the absolute peak velocity.

V. Conclusion

With this case study it has been shown that it is possible to use the 3D PIV technique to obtain quantitative descriptions of large-scale flows in industrial testing environments. The wind tunnel measurements have been conducted in the Aero-acoustic Wind Tunnel (AWT) of the Netherlands Aerospace Center (NLR) on a 1:12 scaled G500 thrust reverser model. The three-dimensional flow field around the nacelle in a thrust reverser configuration encompassing a domain of 0.4 m^3 has been measured using HFSB as flow tracers, three cameras arranged in a line configuration and a laser to illuminate the particles. The flow measurements have been carried out at free-stream velocities of 3-5 m/s and NPRs of 1.0015-1.012 in double-frame mode. Flow seeding was achieved with a specially designed rake from inside the nacelle. The bubble production was stable at 0.45 mm diameter. Testing was completed in minimal time under normal wind tunnel operating conditions. The data processing was done with the 3D Lagrangian particle tracking algorithm Shake-the-Box, and the statistical analysis performed within cubic bins to map the velocity information onto a Cartesian grid. From the image processing and measurement uncertainty analysis it can be concluded that the jet was described to a high degree of spatial resolution and measurement accuracy.

The measurements have been successful in characterizing the three-dimensional nature of the reversed jet. The large-scale structures developing in the flow around the TR such as flow reversal and reverse jet plume recirculation due to the ground effect have been visualized. The jet reversal characteristics with varying free-stream velocity and NPR have been quantitatively mapped. Possible improvements for future tests include: improved optical access around the region of interest; advancement in the statistical analysis of sparse instantaneous velocity data; the uniform seeding of the entire domain.

Acknowledgments

The contributions of Jaap Cornelissen and Arjan Pleijsier to the successful carrying out of the experimental campaign are kindly honored.

References

[1] Van Hengst, J., "Aerodynamic Integration of Thrust Reversers on the Fokker 100", *AGARD 498,* Vol. 10, Texas, United States,1992, pp. 9

[2] Asbury, S., and Yetter, J., "Static Performance of a Wing-Mounted Thrust Reverser Concept", *AIAA*, 1998, pp. 3256 doi: 10.2514/6.1998-3256

[3] Burgsmueller, W., Castan, C., Kooi, J. and Becle, J., "Recent Developments in Low-Speed TPS-testing for Engine Integration Drag and Installed Thrust Reverser Simulation" *AGARD 485*, Texas, United States, 1992, pp.15

[4] Bryanston-Cross, P. and Sale, R., "The Quantitative Visualization of the Flow in a 1/10th Scale Model Thrust Reverser at the Aircraft Research Association, Bedfort," *International Gas Turbine and Aeroengine Congress and Exposition*, ASME, Cologne, Germany, 1992 doi: 10.1115/92-GT-233

[5] Amin, N.F. and Richards, J., "Thrust Reverser Exhaust Plume Reingestion Model Tests", *Journal of Aircraft*, Vol. 21, 1984, pp. 401

[6] Scarano, F., Ghaemi, S., Caridi, G., Bosbach, J., Dierksheide, U. and Sciacchitano, A., "On the use of helium-filled soap bubbles for large-scale tomographic PIV in wind tunnel experiments", *Exp. Fluids*, Vol. 56, 2015, pp. 42. doi : 10.1007/s00348-015-1909-7

[7] Faleiros, D. E., Tuinstra, M., Sciacchitano, A., and Scarano, F., " Generation and control of helium-filled soap bubbles for PIV", *Exp. Fluids*, Vol. 60, 2019, pp.929. doi : 10.1007/s00348-019-2687-4

[8] Gibeau, B., and Ghaemi, S., "A modular, 3D-printed helium-filled soap bubble generator for large-scale volumetric flow measurements", *Exp. Fluids*, Vol. 59, 2018, pp. 178

[9] Faleiros, D. E. "Soap bubbles for large-scale PIV: Generation, control and tracing accuracy", Ph.D. Dissertation, Aerospace Engineering Dept., Delft University of Technology, Delft, 2021

doi : 10.4233/uuid:c579128f-9e96-4e9e-9997-6ce9486e1e25
[10] van Oudheusden, B.W., „PIV-based pressure measurement“, *Meas. Sci. Technol.* Vol. 24, 2013, pp. 1-32
doi : 10.1088/0957-0233/24/3/032001
[11] Jux, C., Sciacchitano, A., Schneiders, J.F.G and Scarano, F., “Robotic volumetric PIV of a full-scale cyclist”, *Exp. Fluids*, Vol. 59, 2017, pp. 74.
doi : 10.1007/s00348-018-2524-1
[12] Schneiders, J. F. G., Scarano, F., Jux, C., and Sciacchitano, A., “Coaxial volumetric velocimetry”, *Meas. Sci. Technol.* Vol. 29, 2018, pp. 065201
doi : 10.1088/1361-6501/aab07d
[13] Sciacchitano, A., Giaquinta, D., Schneiders, J.F.G., Scarano, F., van Rooijen B. D. and Funes, D.E., “Quantitative Flow Visualization of a Turboprop Aircraft by Robotic Volumetric Velocimetry”, *18th International Symposium on Flow Visualization*, Zurich, Switzerland, 2018
[14] Vidales, R.D., “Air-wake flow dynamics on a simplified frigate shape, an experimental study by large-scale tomographic PTV”, M.Sc. thesis, Aerospace Engineering Dept., Delft University of Technology, Delft, 2016
[15] Raffel, M., Kaehler, C. J., Willert, C. E., Werely, S. T., Scarano, F., Kompenhans, J., „*Particle Image Velocimetry*“ 3rd ed., Springer-Verlag, 2018, Chap. 19, pp. 638
[16] Wieneke, B., “Volume self-calibration for 3D particle image velocimetry”, *Exp. Fluids,* Vol. 45, 2008, pp.549.
doi: 10.1007/s00348-008-0521-5
[17] Schanz, D., Gesemann, S., and Schroeder, A., “Non-uniform optical transfer functions in particle imaging: calibration and application to tomographic reconstruction”, *Meas. Sci. Technol.* Vol. 24, 2013, pp. 024009.
doi: 10.1088/0957-0233/24/2/024009
[18] Sciacchitano, A., Scarano, F., “Elimination of PIV light reflections via a temporal high pass filter”, *Meas. Sci. Technol,* Vol. 25, 2014, pp. 084009
doi: 10.1088/0957-0233/25/8/084009
[19] LaVision. (2020). FlowMaster Shake-the-Box: *Product manual*. Goettingen
[20] Aguera, N., Cafiero, G., Astarita, T. and Discetti, S. “Ensemble 3D PTV for high resolution turbulent statistics”, *Meas. Sci. Technol.*, Vol. 27, 2016, pp. 124011
doi : 10.1088/0957-0233/27/12/124011
[21] Schnurr, N. M., Williamson, J. W., and Tatom, J. W., „An Analytical Investigation of the Impingement of Jets on Curved Deflectors“, *AIAA*, Vol. 10, 1972, pp. 1430
[22] Sapkaya, T. and Hiriart, G., “Analysis of Curved Target-Type Thrust Reversers”, *AIAA*, Vol. 13, No. 2, 1975, pp. 185
[23] Strash, D. J., Summa, J. M., Frank, J. H. and Standish, R., “Aerodynamic Analysis of an Installed Thrust Reverser”, AIAA, 1997
doi : 10.2514/6.1997-3153
[24] Caridi GCA, Ragni D., Sciachittano A., and Scarano, F., “HFSB-seeding for large-scale tomographic PIV in wind tunnels,” *Exp. Fluids*, Vol. 57, No. 11, 2016, pp. 190
doi: 10.1007/s00348-016-2277-7
[25] Caridi GCA, “Development and application of helium-filled soap bubbles for large-scale PIV experiments in aerodynamics”, Ph.D. Dissertation, Aerospace Engineering Dept., Delft University of Technology, Delft, 2018